

3D Wavelet Network and Wavelet Transform Used for Transmission Lines Fault Detection and Their Classification

Wael Hussein Zayer
Electronic, Southern Technical University, Amara, Iraq

Abstract: Accurate detection and classification of transmission line faults for permanent protection in avoiding costly maintenance remain challenging to power system engineers. To resolve this issue, we used Wavelet Transform (WT) and 3D-Wavelet Network (3DWN) to detect and classify various types of faults in transmission lines depending on the emanating waves from the power system. First, the WT was used to extract the vector features for each type of faults. Next, these features were analyzed using three level decompositions. The wavelet toolbox in MATLAB/Simulink was utilized to calculate the maximum norm values, maximum detail coefficients and energy of the current signals. Furthermore, 3DWN was employed to classify the single line to ground faults, line-to-line faults, double line to ground faults and three lines faults. Result obtained using WT and 3DWN confirmed the possibility of developing an accurate fault classification scheme useful for reliable transient-based protection approaches where this applicable for each case of faults.

Key words: Transmission line, fault detection, classification, WT, 3DWN, decompositions

INTRODUCTION

Transmission and distribution networks in power system play paramount role towards uninterrupted and safe operations (Osman and Malik, 2001). Power utility companies assure their users to provide continuous power supply where in identifying and locating various types of faults promptly to protect the power system is a priority (Osman and Malik, 2001). To attain such goal it is essential to prevent complete power black outs and maintain secure function of power systems. Modern power utilities demand an efficient scheme to protect the power system and the associated equipments to improve the performance under normal as well as anomalous or faulty operational settings. Over the years, various techniques have been developed to detect fault disturbances in the transmission lines (Osman and Malik, 2001).

Diverse types of faults can occur in the transmission lines with varied distances. Essentially, faults crop up when one, two or more conductors come in contact with each other or ground. The generated faults are classified as single line-to-ground, line-to-line, double line-to-ground and three-phase (Osman and Malik, 2001). Occurrences of these faults in the transmission lines are not only detrimental for expensive electrical equipments but also, responsible for power quality deterioration. Therefore, it is mandatory to determine the nature and location of fault on the line. This in turn helps the engineers for taking remedial measure for prompt

clearance of faults to avoid severe damages. Successful and hazard free operation as well as the durability of power system are majorly decided by the prompt detection and clearance of the faults (Osman and Malik, 2001). Wavelet Transform (WT) being a very effective mathematical tool for detecting time dependent fault-generated signals was widely utilized in several applications of signal processing (Daubechies, 1992). Despite many dedicated efforts precise detection and in-depth classification of diverse faults in transmission lines using simple approaches are far from being achieved.

This study reports the detection of various types of faults that occurs in the transmission lines and their subsequent classification via. three levels decomposition mediated WT. Quantities such as maximum norm, maximum detail coefficients and the energy of the current signals were calculated. Computed values of these parameters in each transmission line for all types of faults were further fed to the proposed 3D-wavelet network to classify the detected faults.

Wavelet transform: Detection and classification of transmission line faults in the power system involves an exceedingly large data set with varied fault situations. In this regard, WT being a handy tool can deal with such circumstances (Osman and Malik, 2001). In WT technique, fault disturbances in power system are usually detected from the alterations in the signal. Wavelet method is more powerful in processing the stochastic signal than

conventional approaches because in WT the waveform are analyzed in the time domain (Daubechies, 1992). Using diverse scale factors, the band in WT can desirably be adjusted to window both the low and high frequency components of the signal. Considering these benefits, WT has widely been used in signal processing applications including de-noising, filtering and image compression. Many pattern recognition algorithms were developed based on the WT. Furthermore, depending on the used scale factors the wavelet can be categorized into different sections (Osman and Malik, 2004).

Generally, WT technique involves the decomposition of transients into a series of wavelet components where each such component corresponds to a time domain signal, covering a specific octave frequency band that contains more detailed information (Shaaban and Hiyama, 2010). Such wavelet components are effective for the detection and classification of the sources of surges. Thus, the WT emerged as a feasible and practical approach for analyzing power system transients and disturbances (Osman and Malik, 2004).

Wavelet transform owing to its capacity of performing multi-resolution analysis (Shaaban and Hiyama, 2010) can efficiently be implemented using High Pass (HP) and Low Pass (LP) filters at level (k) for fundamental frequency components generation (Daubechies, 1992). These results are down-sampled by a factor of two. Same filters are applied to the output of the low pass filter from the preceding stage of the signal. The HP filter is derived from the mother wavelet function directly to measure the details in a certain input. Conversely, the LP filter delivers a smoothen version of the input signal that is extracted from a scaling function associated to the mother wavelet as depicted in Fig. 1. Results for the signal analyses are obtained using DB4 as the mother wavelet. The wavelet energy is the sum of

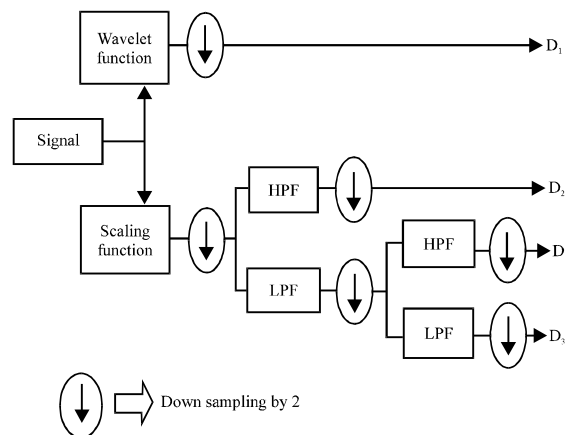


Fig. 1: Multi-resolution analyses

square of detailed wavelet transform coefficients. The energy of wavelet coefficient is varied over different scales depending on the input signals. Energy of the signal is contained mostly in the approximate part and a little in the detail part. Actually, the approximate coefficient at the first level has higher energy than other coefficients at that level of decomposition tree. It is because the faulty signals have high frequency DC components and harmonics that more distinctive to use energy for detail coefficients (Sahu and Sharma, 2013).

MATERIALS AND METHODS

Proposed 3D wavelet network: Figure 2 illustrates the work-flow of 3D Wavelet Network (3DWN) where the input layer is comprised of three neurons because of the three dimensional nature of the input data. The activation function of the input data is one even for three dimensional characters. The first hidden layer is composed of six neurons with each pair taking the minimum value. Then, it reaches to the same neuron in the second hidden layer for selecting the output in the output layer.

The activation functions of the neurons in the first hidden layer must be different. Besides, the three dimensional functions and the activation functions on the second hidden layer should be dissimilar. The one dimensional function is selected depending on the characteristics of the input data. These functions are very significant in order to attain the goal in minimum time without computational complexity. The output layer is consisted of one neuron and the activation function is the summation of the input to it. Meanwhile, the

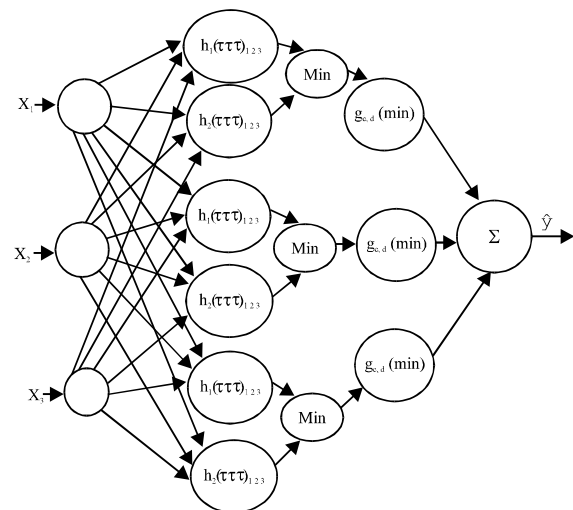


Fig. 2: Block diagram showing the proposed algorithm of 3DWN

weights between the input and the hidden layer are equal to one. Moreover, the weights between the second hidden layer and the output layer are modified according to the specified equations (Jana *et al.*, 2012).

Proposed 3DWN algorithm: The 3DWN architecture approximated any desired signal (y) by generalizing a linear combination of two set of daughter wavelets denoted as $h_{1,a,b}(x_1-x_3)$ and $h_{2,a,b}(x_1-x_3)$ generated by dilation (a) and translation (b) factors from two mother wavelets, $h_{1,a,b}(\tau_1, \tau_2, \tau_3)$ and $h_{2,a,b}(\tau_1, \tau_2, \tau_3)$ respectively with $\tau_1 = x_1-b/a$, $\tau_2 = x_2-b/a$ and $\tau_3 = x_3-b/a$. The expressions for the daughter wavelets yields:

$$h_{1,a,b}(x_1, x_2, x_3) = h_1\left(\frac{x_1-b}{a}, \frac{x_2-b}{a}, \frac{x_3-b}{a}\right) \quad (1)$$

$$h_{2,a,b}(x_1, x_2, x_3) = h_2\left(\frac{x_1-b}{a}, \frac{x_2-b}{a}, \frac{x_3-b}{a}\right) \quad (2)$$

where, $a > 0$ and (x_1-x_3) are the respective maximum norm, maximum detail coefficients and the energy. The 3DWN was consisted of three layers feed forward neural network. First, the 3DWN parameters, dilation factors (a), translation factors (b) and weights (w) should be initialized. Meanwhile, the desired datasets, the input signal (x), the desired output (target, y), the number of scaling functions ($p = 2$ in the present research) and the number of wavelons ($k = 3$ in the proposed method) were inputted. Furthermore, it was assumed that the network output function satisfied the admissibility condition and the network sufficiently approximated the target. The approximated signal of the network (\hat{y}) can be represented via. (Zayer, 2011):

$$\hat{y}(x_1, x_2, x_3) = \sum_{i=1}^k w_i g_{c_i, d_i}(\text{Min}) \quad (3)$$

Where:

- (x_1, x_2, x_3) = The three dimensional data sets
- W_i = The Weight coefficients between hidden and output layers
- i = 1, 2, ..., k (number of wavelons in second hidden layer)
- g_{c_i, d_i} = A daughter wavelets

Similar to WN, the training of 3D WN was started after constructing the initial 3DWN and computing the output signal of the network. It was further trained by the gradient descent algorithm called Least Mean Squares (LMS) to minimize the mean-squared error. During the learning process, the parameters of the network were optimized.

The 3DWN parameters ($a_{j,i}$ and $b_{j,i}$) in the first hidden layer was optimized in the LMS algorithm by minimizing a cost function or the Energy function (E) over all function interval using the expression:

$$E = \frac{1}{2} \sum_{t=1}^T e^2 \quad (4)$$

$$E = \frac{1}{2} \sum_{t=1}^T (y - \hat{y})^2 \quad (5)$$

Where:

$y(x)$ = The desired output (target)

$\hat{y}(x)$ = The actual output signal of 3DWN

The method of steepest descent was used to minimize E which required the gradients such as $\partial E / \partial a_{j,i}$ and $\partial E / \partial b_{j,i}$ for updating the incremental changes to each particular $a_{j,i}$ and $b_{j,i}$ respectively. The gradients of E took the form:

$$\frac{\partial E}{\partial b_{j,i}} = - \sum_{t=1}^T E \times \frac{\partial h(\tau_1, \tau_2, \tau_3)}{\partial b_{j,i}} \quad (6)$$

$$\frac{\partial E}{\partial a_{j,i}} = - \sum_{t=1}^T E \times (\tau_1, \tau_2, \tau_3) \frac{\partial h(\tau)}{\partial b_{j,i}} = (\tau_1, \tau_2, \tau_3) \frac{\partial E}{\partial b_{j,i}} \quad (7)$$

$$\tau_1 = \frac{x_1 - b_{j,i}}{a_{j,i}}, \tau_2 = \frac{x_2 - b_{j,i}}{a_{j,i}} \text{ and } \tau_3 = \frac{x_3 - b_{j,i}}{a_{j,i}} \quad (8)$$

The incremental changes (Δa and Δb) of each coefficient were simply the negative of their gradients as depicted in Eq. 9:

$$\Delta b = - \frac{\partial E}{\partial b} \quad (9)$$

$$\Delta a = - \frac{\partial E}{\partial a} \quad (10)$$

Thus, each coefficient b and a of the network was updated following the rule given by:

$$b(t+1) = b(t) + \mu_b \Delta b \quad (11)$$

$$a(t+1) = a(t) + \mu_a \Delta a \quad (12)$$

where, ($\mu_b = \mu_a = 0.1$ or < 1). The training algorithm of the proposed 3DWN was comprised of the following six steps:

Step 1: Initialization of all three parameters for $p = 2$ and two mother wavelets filters.

$$\left[h_1 \left(\frac{x_1 - b_1}{a_1}, \frac{x_2 - b_1}{a_1}, \frac{x_3 - b_1}{a_1} \right), h_2 \left(\frac{x_1 - b_1}{a_1}, \frac{x_2 - b_1}{a_1}, \frac{x_3 - b_1}{a_1} \right) \right]$$

The desired sets of data, the input signals (x_1 - x_3) the desired output (target y) and the number of wavelets (equal to 3).

Step 2: Setting the number of trainings (iter = 0), the incremental changes of each coefficient (Δa and $\Delta b = 0$) and the initial square error (E_{iter} or <1).

Step 3: Calculation of the approximate network signal (\hat{y}) using Eq. 3.

Step 4: Calculation of the gradients of each coefficient using Eq. 6 and 7. Use Eq. 3 to evaluate the incremental changes of coefficients that are being negative of their gradients.

Step 5: Choosing constants μ_b , $\mu_a = 0.1$ and calculating the new coefficients b_{iter+1} and a_{iter+1} of the network in accordance with Eq. 11 and 12.

Step 6: Calculation of the square error E_{iter+1} using Eq. 5. If E_{iter+1} was sufficiently small (as required or reach the desired value) then the training was good and the execution was stopped. Otherwise, iter = iter+1 was set and moved on to step 3.

In the second hidden layer, the method of steepest descent was used to minimize E which required the gradients $\partial E / \partial w_i$, $\partial E / \partial c_i$ and $\partial E / \partial d_i$ for updating the incremental changes to each particular parameter w_i , c_i and d_i , respectively. The gradients of E are given by:

$$\frac{\partial E}{\partial w_i} = - \sum_{\tau=1}^T E \times g(\tau) \quad (13)$$

$$\frac{\partial E}{\partial d_i} = - \sum_{\tau=1}^T E \times w_i \frac{\partial g(\tau)}{\partial d_i} \quad (14)$$

$$\frac{\partial E}{\partial c_i} = - \sum_{\tau=1}^T E \times w_i \tau \frac{\partial g(\tau)}{\partial d_i} = \tau \frac{\partial E}{\partial d_i} \quad (15)$$

With:

$$\tau = \frac{\text{Min-}d_i}{c_i} \quad (16)$$

The derivatives of the various wavelet filter $\partial g(\tau) / \partial d_i$ with respect to its translation were given. The incremental changes of these coefficients were simply the negative of their gradients expressed as:

$$\Delta w = - \frac{\partial E}{\partial w}, \Delta d = - \frac{\partial E}{\partial d}, \Delta c = - \frac{\partial E}{\partial c} \quad (17)$$

The coefficients such as w_i , c_i and d_i of the WN were updated according to the following rules:

$$\begin{aligned} w(n+1) &= w(n) - \eta_w \Delta w \\ d(n+1) &= d(n) - \eta_d \Delta d \\ c(n+1) &= c(n) - \eta_c \Delta c \end{aligned} \quad (18)$$

where, η is the fixed learning rate parameter. The incremental changes of each coefficient were simply the negative of their gradients as in Eq. 18. Thus, each coefficient w , d and c of the network was updated in following the rule given in Eq. 13-15. The training algorithm of the second hidden layer parameters were obtained via the following six steps.

Step 1: Initialization of the parameters such as dilation (c), translation (d) and weight (w), $p = 1$, two mother wavelets filters $[g(\text{min-}d/c)]$ the desired datasets, the input signal (x), the desired output (target, y) and the number of wavelets (equal to 3).

Step 2: Setting the number of trainings (iter = 0), the incremental changes of each coefficient (Δw , Δc , $\Delta d = 0$) and the initial square error ($E_{iter} = 0.1$).

Step 3: Calculation of the approximate network signal (\hat{y}) using Eq. 3.

Step 4: Calculation of the gradients of each coefficient using Eq. 13-15. Use of Eq. 18 to compute the incremental changes of coefficients those is negative of their gradients.

Step 5: Selection of constants η_w , η_d , $\eta_c = 0.1$ and calculation of the new coefficients w_{iter+1} , d_{iter+1} and c_{iter+1} of the network according to the rules provided in Eq. 18.

Step 6: Calculation of the square error E_{iter+1} using Eq. 5. If E_{iter+1} was small enough (as required or reach the desired value $E_{iter+1} = 0.001$) then the training was good and the program execution was stopped. Otherwise, iter = iter + 1 was set and moved onto step 3. Figure 2 displays the working mechanism of the 3DWN training algorithm.

Transmission line: In every electric power system, overhead transmission lines constitute the main components that connect the generating stations and load centers. Often, these lines are hundreds of kilometers long because the generating stations are far away from the load centers. However, these lines must be isolated immediately because occurrences of faults can destabilize the power system results in power black outs. Faults analyses are extremely crucial in power system engineering to clear them quickly for immediate power

Table 1: Model parameters of the power system for constant $f = 50$ Hz, $V = 400$ V and $L = 300$ km

$Z(\Omega)$	$Y(\Omega)$	$C(nF/km)$
$R1 = 1.31$	$R1 = 8.25$	$C1 = 13.0$
$R2 = 2.33$	$R2 = 82.5$	$C2 = 8.50$
$X1 = 15.0$	$X1 = 94.5$	-
$X2 = 26.6$	$X2 = 308.0$	-

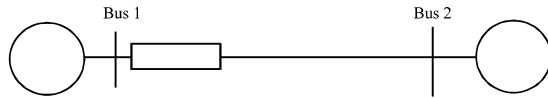


Fig. 3: A model for single line diagram representing the power system

supply restoration without any interruption. Thus, the detection of faults and locating them accurately is essential for necessary repairs and to avoid permanent damages of power system. In fact, the quality of the power delivery is affected by the time required to locate the fault point along the transmission line. Protection of transmission lines is a significant issue in power system engineering because ≈ 85 - 87% of faults in power system are occurred in the transmission lines (Borkhade, 2014).

Model description: Following the earlier research by Borkhade (2014) present a study used the same model wherein the single line diagram of the simulated power network was used as indicated in Fig. 3. The power system was consisted of two sources A and B with buses 1 and 2 separated by a transmission line of Length (L) 300 km. Table 1 enlists various model parameters such as sources Voltage (V), frequency (f), Capacitances (C), impedances of the sources (Z) and transmission lines (Y) used.

Fault classification using 3DWT: The output of the wavelet transform after three levels decomposition (Daubechies, DB4) was selected as mother wavelet. The time resolution of DB4 was accurate for providing the fast transients induced by faults. Maximum norm values, maximum detail coefficient and energy of the current signal were calculated from the wavelet toolbox in MATLAB/Simulink. These values were used for feature extraction of signals. The WT was mainly advantageous in attaining sufficient information about the signal with minimal vector dimension. It could decompose current and voltage signals in the time and frequency domain to detect the fault accurately.

The vector of feature extraction (maximum norm values, maximum detail coefficient and energy of the current signal) for each line was then entered as input to the 3DWN to train and adapt an excellent pattern recognition, classification and generalization. The 3DWN

structure consisted of input layer having three nodes that was fed by the feature vector of three phases at each type of fault. Input nodes were fully interconnected with the first hidden layer where the hidden nodes had the activation function. First hidden layer was not fully interconnected with the second hidden layer that had one dimension activation function. The second hidden layer was fully interconnected with the output node.

The input features were (x_1 : maximum norm of phase A, maximum norm of phase B and maximum norm of phase C) (x_2 : maximum detail coefficient of phase A, maximum detail coefficient of phase B and maximum detail coefficient of phase C) and (x_3 : energy of the current signal for phase A, energy of the current signal for phase B and energy of the current signal for phase C). The target of the 3DWT for fault classification under normal condition were varied from 1-11 with corresponding faults of LA-G, LB-G, LC-G, LL-AB-G, LL-AC-G, LL-BC-G, LL-AB, LL-AC, LL-BC and LLL.

Training of 3DWT: Input feature vector of each signal was provided for adapting the network according to the target. Five different positions for each fault were considered to adapt the network. Then, these were saved as the weight (w_1 - w_3) in a matrix with dimensions of (15×11) where ($15 = 5 \times 3$). The feature matrix included 5 positions, 3 weights and 11 faults.

Testing of 3DWT Any signal to be tested was entered in the 3DWN and its weights vector was compared with the feature vectors matrix. The results were obtained by determining the correlation between these vectors. The maximum value of correlation implied the representation of faults feature where the value of maximum correlation place was in its column.

RESULTS AND DISCUSSION

Analysis of simulation results

Normal condition: Figure 4 shows the three-phase current and voltage signals (color of A is red, B is blue and C is yellow) at no fault condition. In the absence of any fault, the detail coefficients for all three phases were found to be close to zero and only appeared as ending effect of daubechies wavelet which was very small. The values of energy of the signal, maximum norm and maximum detail coefficient for normal condition are summarized in Table 2.

Single phase to ground fault: Three-phase current and voltage signals for phase A to ground fault is illustrated in

Table 2: Values of Maximum Detail Coefficient (MDC), Maximum Norm (MN) and Energy (E) of three phases A-C at normal condition

A			B			C		
MDC	E	MN	MDC	E	MN	MDC	E	MN
0.358	79.12	0.433	0.4585	80.72	0.433	0.3195	81.6	0.433

Table 3: Values MDC, MN and E of three phases A-C at single phase to Ground (G) Fault (F)

F	A			B			C		
	MDC	E	MN	MDC	E	MN	MDC	E	MN
A-G	0.923	188.540	3.874	0.123	78.43	0.585	0.135	81.54	0.5853
B-G	0.285	99.452	0.348	2.423	209.60	4.207	0.362	103.90	0.339
C-G	0.315	92.112	0.420	0.221	90.36	0.411	0.924	195.90	5.018

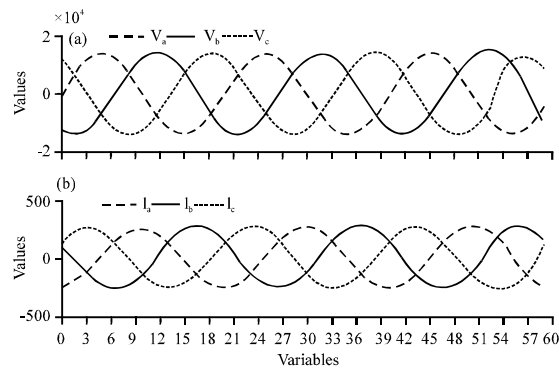


Fig. 4: Phase voltage and current at normal condition

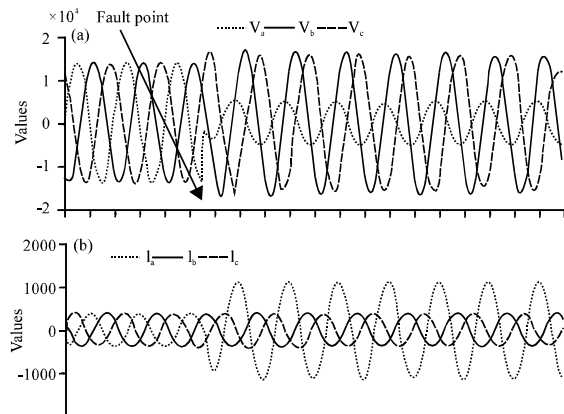


Fig. 5: Phase voltage and current at line to ground fault

Fig. 5. The values of detail coefficients revealed that the fault inception began at the instant fault occurred on phase A without altering other phases compared to phase A. The values of energy of the signal, maximum norm value and maximum detail coefficient for line to ground condition are presented in Table 3. Because the faulty phase maximum norm value, energy of signal and

Table 4: Values MDC, MN and E of three phases A-C at double phases to ground fault

F	A			B			C		
	MDC	E	MN	MDC	E	MN	MDC	E	MN
AB-G	0.908	195.420	4.458	0.881	177.500	4.521	0.321	81.50	1.652
BC-G	0.211	86.856	1.332	0.839	179.930	5.021	0.812	184.20	5.161
CA-G	0.791	191.640	4.619	0.331	83.643	1.594	0.753	186.32	4.602

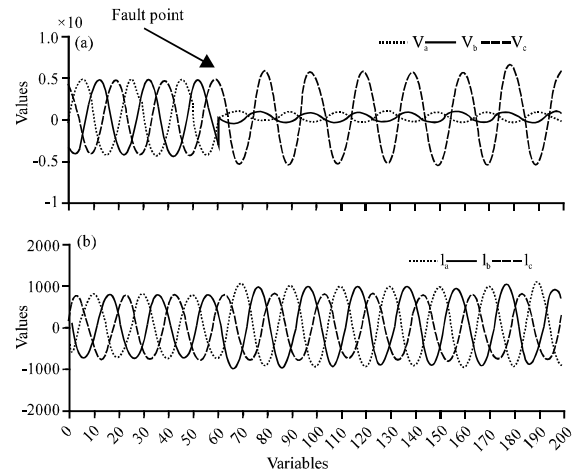


Fig. 6: Phase voltage and current for line to ground fault

maximum detail coefficients was highest, thus, it was needed to be cleared immediately upon detection in the transmission line.

Double phase to ground fault: Three phase current and voltage signals with phases A-B to ground fault are shown in Fig. 6. In this case, only two faulty phases at the fault inception time caught a substantial change and high level of detail coefficient despite no change in the healthy phase (Table 4). Literally no change in the healthy phase could maintain nearby normal condition in the energy and maximum norm, although, faulty phases were so different. It implied that these phases were in fault condition and when making the maximum detail coefficients for two faulty phases were different (not identical). This indicated that these faulty phases were connected to the ground of transmission line.

Double phase fault: Figure 7 depicts the three phase current signals with phases A-B fault. Only two faulty phases at fault time was found to catch substantial alteration, although, the healthy phase had nearly zero change Table 5. No change in the healthy phase and maintenance of nearby normal condition in the detail coefficient, energy and the change of energy ratio clearly indicated that the faulty phases were very different than normal condition where the maximum detail coefficient of

Table 5: Values MDC, MN and E of three phases A-C at double phases fault

F	A			B			C		
	MDC	E	MN	MDC	E	MN	MDC	E	MN
AB	0.213	180.210	5.92	0.307	178.430	5.890	0.25	82.456	0.301
BC	0.361	77.442	0.45	0.281	184.210	3.980	0.34	180.371	3.582
CA	0.411	187.320	5.01	0.369	76.981	0.421	0.39	190.027	4.790

Table 6: Values MDC, MN and E of three phases A-C at three phases fault

F	A			B			C		
	MDC	E	MN	MDC	E	MN	MDC	E	MN
ABC	0.481	180.561	5.382	0.502	185.45	4.98	0.378	184.93	4.839

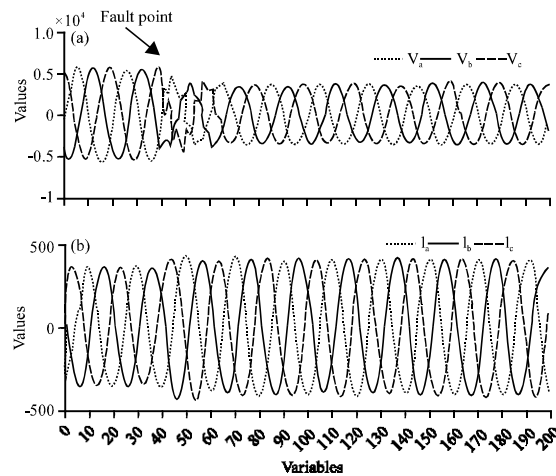


Fig. 7: Phase voltage and current for 3-line to ground fault

these faulty phases were found to be above 0.001. It implied that these phases were in fault condition and when making compression the amount of energy change ratio of two faulty phases were typically same (negligible difference). This clearly indicated that the occurred faulty phases were not connected to the ground.

Three phase fault: Figure 7 presents the three phase current and voltage signals with three phase fault. In this case, at fault inception time a great changes were observed in all phases energy, maximum norm values and maximum detail coefficients as described in Table 6.

CONCLUSION

We applied WT and 3DWN to detect and classify various types of faults appeared in the transmission line. WT could detect the faults accurately by decomposing

the signal into bands in the time and frequency domain. Values of maximum norm, maximum detail coefficients and the energy of the current signal were calculated using wavelet toolbox within MATLAB/Simulink. These values were further fed to the proposed 3DWN algorithm. 3DWN provided very good classification and was robust than other types of classifiers. Result obtained using WT and 3DWN confirmed the possibility of developing an accurate fault classification scheme useful for reliable transient-based protection approaches. The performance of the proposed classifier was evaluated by altering the network configuration. It was concluded that the developed scheme was easily comprehensible, deterministic and feasible for practical implementation.

REFERENCES

- Borkhade, A.D., 2014. Transmission line fault detection using wavelet transform. *Intl. J. Recent Innovation Trends Comput. Commun.*, 2: 3138-3142.
- Daubechies, I., 1992. *Ten Lectures on Wavelets*. Vol. 61, Society for Industrial Applied Maths, Philadelphia, pp: 357.
- Jana, S., S. Nath and A. Dasgupta, 2012. Transmission line fault classification based on wavelet entropy and neural network. *Intl. J. Electr. Eng. Technol.*, 3: 94-102.
- Osman, A.H. and O.P. Malik, 2001. Wavelet transform approach to distance protection of transmission lines. *Proceedings of the International Conference on Power Engineering Society Summer Meeting Vol. 1*, July 15-19, 2001, IEEE, Vancouver, Canada, ISBN:0-7803-7173-9, pp: 115-120.
- Osman, A.H. and O.P. Malik, 2004. Protection of parallel transmission lines using wavelet transform. *IEEE. Trans. Power Delivery*, 19: 49-55.
- Sahu, S. and D.A.K. Sharma, 2013. Detection of fault location in transmission lines using wavelet transform. *Intl. J. Eng. Res. Appl.*, 3: 149-151.
- Shaaban, S.A. and T. Hiyama, 2010. Transmission line faults classification using wavelet transform. *Proceedings of the 14th International Conference on Middle East Power Systems (MEPCON'10)*, December 19-21, 2010, Cairo University, Giza, Egypt, pp: 532-537.
- Zayer, W.H., 2011. *Person identification using face and finger print authentication*. Ph.D Thesis, University of Basrah, Basra, Iraq.